Journal of Non-Newtonian Fluid Mechanics 238 (2016) 233–241

Contents lists available at ScienceDirect

Journal of Non-Newtonian Fluid Mechanics

journal homepage: www.elsevier.com/locate/jnnfm

On different ways of measuring "the" yield stress☆

Maureen Dinkgreve[a,*], José Paredes[a], Morton M. Denn[b], Daniel Bonn[a]

[a] Van der Waals-Zeeman Institute, Institute of Physics, University of Amsterdam, Science Park 904, 1098 XH Amsterdam, The Netherlands
[b] Benjamin Levich Institute and Department of Chemical Engineering, City College of New York, CUNY, New York, NY 10031, USA

ARTICLE INFO

Article history:
Received 7 April 2016
Revised 14 October 2016
Accepted 3 November 2016
Available online 5 November 2016

Keywords:
Yield stress materials
Rheological measurements
Oscillatory measurements
Herschel–Bulkley model

ABSTRACT

Yield stress materials are ubiquitous, yet the best way to obtain the value of the yield stress for any given material has been the subject of considerable debate. Here we compare different methods of measuring the yield stress with conventional rheometers that have been used in the literature on a variety of materials. The main conclusion is that, at least for well-behaved (non-thixotropic) materials, the differences between the various methods are significant; on the other hand, the scaling of the measured yield stress with the volume fraction of dispersed phase shows the same dependence independently of the way in which the yield stress is obtained experimentally. The measured yield strain is similarly found to depend on the method employed. The yield stress values obtained for a simple (non-thixotropic) yield stress fluid are only similar for Herschel–Bulkley fits and stress-strain curves obtained from oscillatory measurements. Stress-strain curves with a continuous imposed stress or strain rate differ significantly, as do oscillatory measurements of the crossover between G′ and G″ or the point where G′ starts to differ significantly from its linear response value. The intersection of the G′ and G″ curves as a function of strain consistently give the highest value of the yield stress and yield strain. In addition, many of these criteria necessitate some arbitrary definition of a crossover point. Similar conclusions apply for a class of thixotropic yield stress materials, with the stress-strain curve from the oscillatory data giving the dynamic yield stress and the Herschel–Bulkley fit either the static or dynamic yield stress, depending on how the measurement is carried out.

1. Introduction

Many materials found in daily life exhibit properties characteristic of either solids or liquids, depending on the imposed stress. At small stresses these materials deform essentially in an elastic manner, but flow once a critical stress is exceeded; this critical value is called the *yield stress* (σ_y), and materials exhibiting a yield stress are called *yield stress materials*. Examples of yield stress materials include concentrated emulsions like cosmetic creams or margarine, toothpaste, foams, polymer gels like Carbopol, slurries, and some composites [13,15,58]. Determining the yield stress is critical in industrial processes; the yield stress is required to know the minimum pressure needed to start a slurry in a pipeline, for example, or to know the stiffness of dairy products [39]. In concrete utilization the yield stress determines whether air bubbles will remain trapped [34].

The notion of a yield stress fluid was introduced by Bingham and coworkers, whose intellectual frame of reference was plastic yielding in metals; see, for example, the discussion in [5,12]. The yield stress for a material that flows with viscous dissipation has thus been defined in an operational manner as the stress at which flow begins, which, as we shall see, can contain ambiguities. Many methods have been proposed for determining the yield stress; it has been demonstrated that variations of more than one order of magnitude can arise, however, depending on the method used and the handling of the sample [28,37,59]. This has led, amongst other things, to the suggestion that there may be two yield stresses, dynamic and static; the former would be given by the minimum stress needed to start a flow and the latter would be the smallest stress applied before a sample stops flowing.

Several works, including [14,25,33,35,42], have proposed that yield stress materials can be classified into two categories: 'simple' and thixotropic. For 'simple' yield stress materials the viscosity depends only on the shear rate, and the yield stress is well defined; the yield stress can therefore be considered a material property. For thixotropic yield stress materials the viscosity depends not only on the shear rate but also on the (deformation) history of the sample, implying that for this type of material the

☆ Presented at Viscoplastic Fluids: From Theory to Application VI, Banff, October 25–30, 2015.

* Corresponding author.
E-mail addresses: maureen.dinkgreve@gmail.com, m.dinkgreve@uva.nl (M. Dinkgreve).

http://dx.doi.org/10.1016/j.jnnfm.2016.11.001
0377-0257/

rheological behavior is given by a competition between aging – spontaneous build-up of some microstructure – and shear rejuvenation – breakdown of the microstructure by flow. (Ovarlez et al. [43] have recently suggested that a third class of yield-stress material exists in which the yield stress can be tuned by an appropriate flow history.) Very recently, Balmforth et al. [3] and Coussot [16] showed that for a 'simple' yield stress material the static and the dynamic yield stresses are indeed the same, while for thixotropic yield stress materials these stresses are different. Our focus in this article is to examine and evaluate various means that have been proposed and used in the literature to determine the yield stress of simple yield stress materials; for completeness, we will also consider what happens if different ways of measuring the yield stress are applied to thixotropic samples. We focus on methods that can be easily implemented on conventional rheometers with no *a priori* estimate of the yield stress.

A classical way of determining σ_y is by means of steady shear measurements, consisting of performing shear rate or shear stress sweeps that lead to steady state flow curves, i.e. shear stress (σ) as a function of the shear rate ($\dot{\gamma}$). The yield stress can then be determined either by direct extrapolation of σ as $\dot{\gamma}$ goes to zero or by fitting the flow curve to a rheological model, such us that proposed by Herschel and Bulkley [26]: $\sigma = \sigma_y + K\dot{\gamma}^n$, where σ_y is the yield stress and K and n are adjustable model parameters. Depending on how the sweeps are performed, i.e. decreasing or increasing shear rate or shear stress sweeps, this technique can be used for determining the dynamic and the static yield stress. One caveat is that, as has been discussed at length in the literature, the accuracy of the extrapolation and the results for different models for determining σ_y depend on the lowest-measured $\dot{\gamma}$ used for the extrapolation [8]. Now, however, commercial rheometers have become sufficiently sensitive that this is no longer a real problem in most practical cases, although extremely long times may be required at the lowest shear rates to ensure that a true steady state has been obtained.

Another method that allows for the determination of both σ_y and the yield strain γ_y is the stress growth experiment, in which a shear rate is imposed and the resulting σ is recorded as a function of time or γ. Typical curves frequently show an initial linear regime corresponding to linear elastic deformation, followed by a deviation from linearity and in some cases by a stress overshoot, after which a steady σ value is reached, as shown, for example, by Barnes and Nguyen [7]. However, different σ_y (and γ_y) can be inferred from the same experiment, depending on how the yield point is defined; i.e. σ_y (or γ_y) has variously been defined by the departure from linearity, by the maximum stress (and the corresponding γ), or by the point at which the stress reaches a constant value; see Møller et al. [34] for a discussion.

Some workers have proposed that the yield stress can be also measured from oscillatory experiments by carrying out a strain sweep at a fixed frequency of oscillation. These measurements consist of imposing a sinusoidal strain of amplitude γ_0 and frequency ω, given by $\gamma(t) = \gamma_0 \sin(\omega t)$. If γ_0 is small enough to satisfy the linearity constraint, i.e. the stress at any time is directly proportional to the value of the strain, then the stress can be represented by Barnes et al. [6] and Larson [30]:

$$\sigma(t) = \gamma_0[G'(\omega)\sin(\omega t) + G''(\omega)\cos(\omega t)] \quad (1)$$

where the storage modulus G′ quantifies elastic (recoverable) deformation and the loss modulus G″ quantifies viscous dissipation. At higher amplitudes, commonly called Large Amplitude Oscillatory Strain, or LAOS, the response becomes nonlinear, higher harmonics occur, and G′, which is the coefficient of the fundamental, does not contain all of the relevant elasticity information.

Oscillatory measurements allow the acquisition of curves of G′ and G″ as functions of either γ or σ. Different authors have proposed a variety of ways of determining σ_y and γ_y from oscillatory measurements: (i) by the point at which $G' = G''$ [e.g., 29,46,49], sometimes called the *characteristic modulus*; (ii) by fitting the behavior well above the yield point with a power-law function and defining the yield point by the intersection of this line with the horizontal line through the linear G′ data [20,52]; or (iii) by plotting σ vs γ on logarithmic coordinates, from which σ_y and γ_y are given by the intersection of a line with unit slope at low strains (corresponding to a linear elastic response, i.e., stress is proportional to strain) with a power-law equation at high strains [18,19,31,53]. (Considering that at small deformations a yield stress material behaves like an elastic solid and $\sigma = G'\gamma$, the line with unit slope on logarithmic coordinates is expected to correspond to G′.) Each of these methods may be sensitive to the imposed frequency.

Mewis and Spaull [32] proposed that yielding seems to occur at a constant shear *strain*, and that it would be preferable to work with a yield strain (γ_y) instead of working with yield stress. If the material responds as an elastic solid prior to yielding then there is a unique yield strain that corresponds to the yield stress, and the two quantities are equivalent. If the unyielded material is a viscoelastic solid, however, then the stress-strain curve prior to yielding is rate dependent and the apparent yield stress would depend on rate for a system that has a fixed yield strain; see, for example, the treatment of Nguyen and Boger's [38] classic yield stress measurements on "red mud" by Denn and Bonn [21]. γ_y may be very small, possibly 10^{-3} or lower (see [32] and references therein), and so it may not always be possible to get an accurate measurement.

Finally. Measurement of the creep compliance has been proposed [e.g., 18] as a definitive way to measure the yield stress: the strain should approach a constant value for imposed stresses below the yield stress, while flow should be initiated and the compliance should become an increasing function of time for stresses above the yield stress. Creep is a fundamentally different type of experiment from the others described here, because it requires *a priori* knowledge of the stress range in which yielding is expected to occur.

In this paper, we use simple and thixotropic yield stress materials to compare the yield stresses and yield strains obtained from steady shear, oscillatory shear, stress growth, and creep experiments. The simple yield stress materials are emulsions, Carbopol gels, a commercial hair gel, and a shaving foam, while the thixotropic materials are emulsions loaded with clay [45,48]. We quantify the difference between different methods and compare them. Some of them necessitate the definition of a crossover point that is not without ambiguity; the scaling of σ_y with the amount of dispersed phase is generally independent of the method used, however.

2. Materials and methods

2.1. Carbopol samples and hair gel

Carbopol is a cross-linked polyacrylic acid that swells in water under neutral pH so that the particles jam together, generating a yield stress fluid [46].

[47] We prepared Carbopol samples by mixing 2 wt% of Carbopol Ultrez U10 grade and ultra-pure water for one hour. The pH of the mixture was adjusted to 7 by adding approximately 20 mL of 18wt% NaOH, and the sample was stirred mechanically at 100 rpm for one hour, then left to rest for one day. The 2 wt% Carbopol sample was diluted with ultra-pure water to obtain samples with 1.5, 1.0, 0.75, 0.5 and 0.1 wt% Carbopol, and the pH was checked in each case.

The hair gel was a commercial product (Albert Heijn). This is basically a Carbopol gel in which the pH is adjusted by using triethanolamine rather than NaOH.

2.2. Emulsions and foam

Castor oil-in-water emulsions were stabilized using sodium dodecyl sulfate (SDS). Castor oil was dispersed in a 1 wt% SDS solution using a homogenizer (Ultraturrax). We prepared a batch of emulsion with internal volume fraction $\phi = 0.8$; from this batch, samples with $\phi = 0.78$, 0.74, 0.70, 0.67 and 0.66 were prepared by dilution with the 1 wt% SDS solution. The mean diameter of the oil droplets is 3.2 µm with 20% polydispersity. It is well know that the system jams if the internal volume fraction of an emulsion is above a critical internal volume fraction $\phi_c \approx 0.645$, thus exhibiting a yield stress, as shown by Paredes et al. [44] using the same system.

The foam was a commercial shaving foam, Gillette Foamy Regular. The liquid volume fraction of the shaving foam was $9.2 \pm 0.5\%$, with a mean bubble radius of about 18 µm, in fair agreement with previously reported data on the same brand [56].

2.3. Thixotropic emulsions

Thixotropic emulsions were prepared by mixing pure castor oil-in-water emulsions ($\phi = 0.78$, 0.74, 0.70, 0.67 and 0.66) with clay (Bentonite, from Steetley) such that the final concentration of clay in all samples was 2 wt%. Clay induces the formation of links between the neighboring droplets in the emulsion, as has been directly visualized by Fall et al. [25], and leads to thixotropy [48].

2.4. Rheological measurements

Our measurements were carried out using a controlled-shear-stress rheometer (CSS, Physica MCR302) and a controlled-shear-rate rheometer (CSR, ARES), both with a 50 mm-diameter cone-and-plate geometry with a 1° cone and roughened surfaces to avoid wall slip [11,33]. Before performing any experiments, samples were pre-sheared at a shear rate of $100\,s^{-1}$ for 30 s, followed by a rest period of 30 s in order to create a controlled initial state in the samples [4,17]. The static normal stresses in all samples were zero after the rest period.

The steady shear experiments were performed with the CSR rheometer by carrying out shear rate sweeps from $100\,s^{-1}$ to $1 \times 10^{-3}\,s^{-1}$ (to 10^{-4} for the oil-in-water emulsions), obtaining flow curves that were fit to the Herschel–Bulkley model. (High-to-low rate sweeps are preferable for systems that exhibit no thixotropy, because short-term transients caused by the transition from viscoelastic solid to mobile liquid at fluidization are avoided.) The oscillatory measurements were performed with the CSS rheometer by carrying out shear stress sweeps from 1×10^{-2} Pa to 5×10^{2} Pa at a constant frequency of 1 Hz, generating curves of G′ and G″ as functions of σ or γ. The linear viscoelastic storage modulus G′ is insensitive to frequency in this range for all materials studied; the linear loss modulus G″ is always much smaller than G′ and is insensitive to frequency for all systems but the emulsion, where there is a transition from a frequency dependence of about $\omega^{1/4}$ to $\omega^{1/2}$ in the neighborhood of 1 Hz. (See Supplementary Material.)

The stress growth experiments were performed with the CSR rheometer by imposing a constant shear rate $\dot{\gamma} = 10^{-2}\,s^{-1}$ and recording σ for 300 s, equivalent to a total deformation $\gamma = 3$. Finally, the creep experiments were carried out with the CSS rheometer with increasing imposed stresses starting near to but below the expected yield stress, as determined by the other measurements. The creep experiments were carried out at a later date, using new samples prepared according to the same protocols; the samples were presheared as described above before each creep measurement.

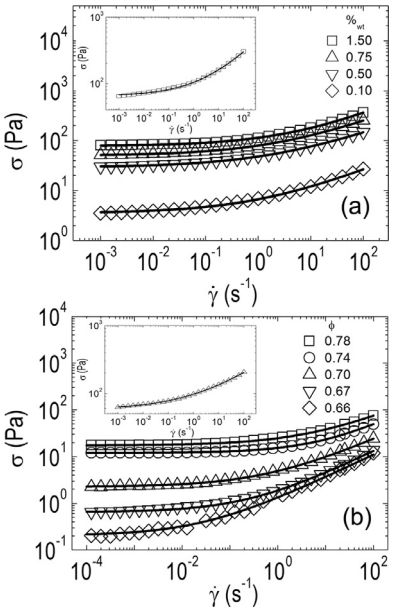

Fig. 1. Flow curves obtained by means of steady shear measurements. (a) Carbopol at different mass concentrations. Inset: Hair gel. (b) Emulsions with different internal volume fractions. Inset: foam. Lines are the fits of the flow curves to the Herschel–Bulkley model.

Given that the appearance of hysteresis in an inelastic or weakly elastic liquid is a hallmark of thixotropy, we performed up-and-down shear rate sweeps on the clay emulsions. First the shear rate sweep was performed from a low to a high shear rate value, followed by a shear rate sweep from a high to a low shear rate value. Previous experiments regarding loaded emulsions, as done by Ragouilliaux et al. [48], Fall et al. [25] and Paredes et al. [45], were performed using highly concentrated systems ($\phi > 0.70$); our loaded emulsions here cover a larger concentration range. The non-thixotropic character of the simple yield stress materials we use has been reported in [25,44], and we do not report up-and-down shear rate sweeps on these materials here.

3. Results and discussion

3.1. Simple yield stress fluids

3.1.1. Rheological measurements

Steady shear measurements. Flow curves obtained for all our simple yield stress materials are shown in Fig. 1. The flow curves are clearly approaching plateaus at low shear rates within the range at which data were obtained, and all can be fit to the Herschel–Bulkley model. (The model fits are based on the range of accessible shear rates, and it is possible that the power-law index might change if higher rates could be explored, but our interest is in the fit to the yield stress, which should be insensitive to rates above $100\,s^{-1}$.)

Oscillatory measurements. Curves of G′ and G″ as functions of σ and γ at a frequency of 1 Hz are shown in Figs. 2 and 3, respectively. At low amplitudes, G′ and G″ are independent of stress magnitude and represent the entire elastic or dissipative contributions, respectively. Higher harmonics appear in the LAOS measurements at larger amplitudes, and the coefficients of the harmonics become strain dependent. The coefficients of the fundamental

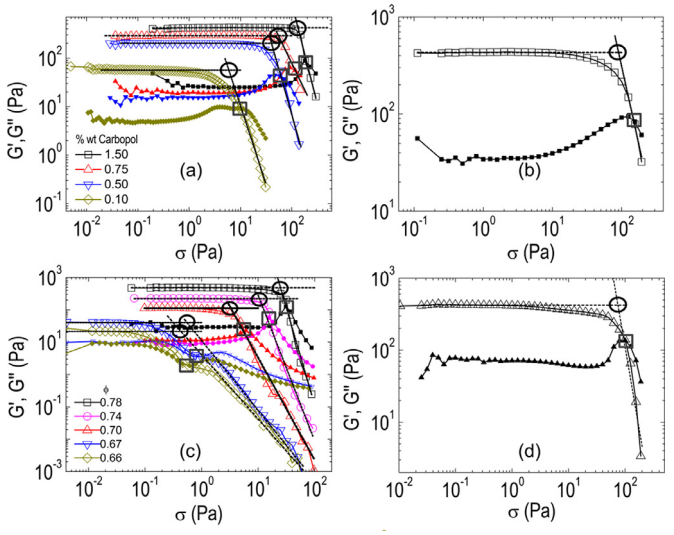

Fig. 2. Storage (G′) and loss (G″) moduli as functions of σ for (a) Carbopol samples, (b) hair gel, (c) emulsions, and (d) foam. Open symbols correspond to G′, filled symbols to G″. Black lines are power-law fits of the behavior well above yield point, whose intersection with the horizontal line through the linear G′ data is shown by the black circles. Gray squares show σ at the characteristic modulus, G′ = G″.

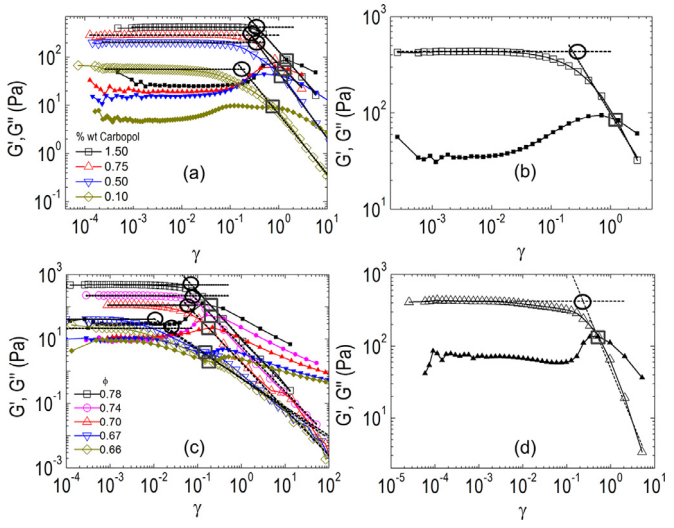

Fig. 3. Storage (G′) and loss (G″) moduli as functions of γ for (a) Carbopol samples, (b) hair gel, (c) emulsions, and (d) foam. Open symbols correspond to G′, and filled symbols correspond to G″. Black lines are power-law fits of the behavior well above the yield point, whose intersection with the horizontal line through the linear G′ data is shown by the black circles. Gray squares show γ at the characteristic modulus, G′ = G″.

(the frequency of the stress or strain input) are still conventionally called G′ and G″, and we follow that convention here, but these functions no longer represent the complete elastic or dissipative portions of the stress in the nonlinear regime. Treatments of the nonlinear data are discussed in, for example, [2,9,24,27,51].

Now, the question is how to extract the yield stress from these data? As noted by Rouyer et al. [52], "*There is no unique and rigorously motivated criterion allowing a yield stress to be determined from oscillatory data.*" For example, Renou et al. [49], Perge et al. [46] and Kugge et al. [29] define the yield stress as the stress for which G′ = G″ (the *characteristic modulus*), where the viscous and the elastic contributions to the fundamental are equal; at higher stresses the viscous contribution will dominate the elastic, indicating that the material is indeed flowing. The location of the characteristic modulus is indicated by gray squares in Figs. 2 and 3. The

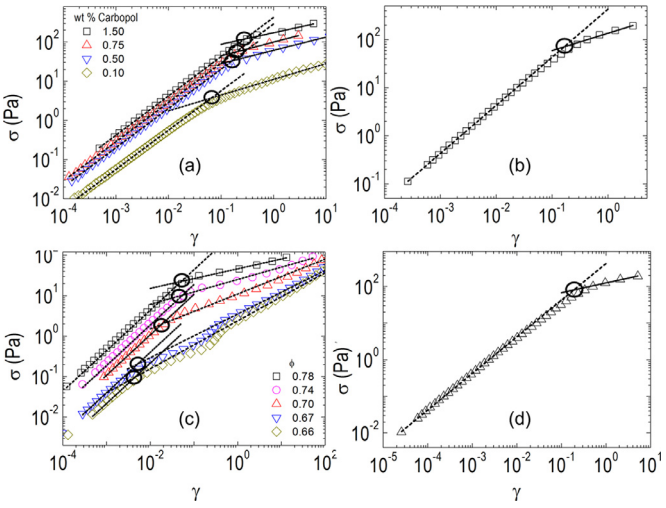

Fig. 4. σ vs γ obtained from the oscillatory measurements (same data shown in Figs. 2 and 3) for (a) Carbopol samples, (b) hair gel, (c) emulsions, and (d) foam. Lines are power-law fits of the behavior well above and well below the yielding point, whose intersection is shown by the black circles.

yield stress and the yield strain can also be defined from this approach by the intersection of the horizontal line representing the behavior of G′ well below the yielding point with the power-law equation representing the behavior of G′ well above the yielding point; this method was used by Rouyer et al. [52] for determining the yield stress of foams. These intersections are shown as dark circles in Figs. 2 and 3. We also re-plot the oscillatory data shown in Figs. 2 and 3 as σ vs. γ (Fig. 4). The data are linear at small strains with a unit slope on log-log coordinates; the magnitude of the line corresponds to G′ in the linear regime. (G′ ≫ G″ in this regime, so the total stress is comprised mostly of the elastic component.) Following Mason et al. [31], Saint-Jalmes and Durian [53] and Christopoulou et al. [18] for similar systems, σ_y and γ_y can then be obtained from the intersection of the line at low strains and a power law drawn through the data at high strains.

These methods employing oscillatory data are empirical and are all based on departures from the linear viscoelastic regime. Only the use of the characteristic modulus is unambiguous; the other methods require extrapolations that will depend on the quality of data and the range selected for fitting a power law. The transitions in the plots of σ vs. γ in Fig. 4 appear sharper to the eye than those of G′ versus σ or γ in Figs. 2 and 3, respectively. One interesting feature of these data for most systems is that the intersection of G′ and G″ as functions of σ occurs at or near the maximum in G″; i.e., the maximum value of G″ is very close to the characteristic modulus.

Stress growth experiments. The evolution of σ as a function of γ at an imposed steady strain rate $\dot{\gamma} = 10^{-2}\,s^{-1}$ is shown in Fig. 5. The stress initially grows with increasing strain in what is an elastic or viscoelastic solid response, followed by a transition to a steady stress that characterizes a fluid response; in some cases there is a stress overshoot. Here, too, there are a number of ways in which the yield stress and yield strain can be defined [7]: (i) the highest σ (or corresponding γ) at which the response is still elastic, (ii) the maximum σ (or corresponding γ), or (iii) the stress at which a steady state is achieved.

Defining the yield point as the highest stress at which the response is still elastic is ambiguous. One approach is to choose the point at which the stress-strain response deviates from linearity, but this depends on the time resolution and the imposed rate. Furthermore, the deviation from linearity might simply be a transition

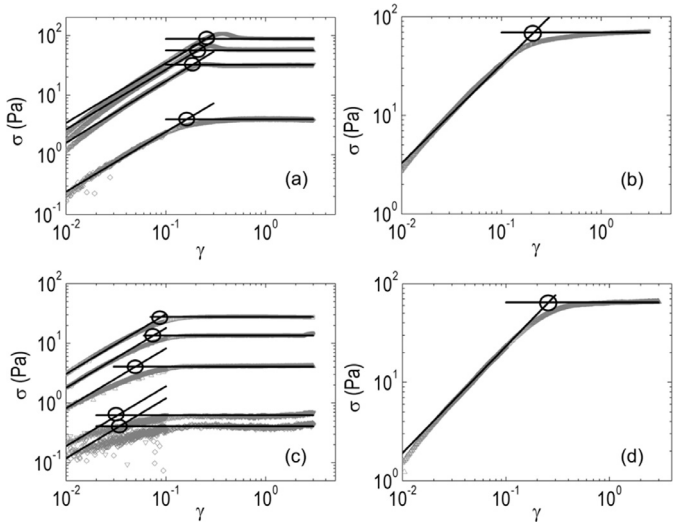

Fig. 5. σ as a function of γ at an imposed $\dot{\gamma} = 1 \times 10^{-2}\,s^{-1}$ for (a) Carbopol samples with wt%-Carbopol: 1.5, 0.75, 0.50, and 0.10 (top to bottom), (b) hair gel, (c) emulsions with $\phi = 0.78$, 0.74, 0.70, 0.67, and 0.66 (top to bottom), and (d) foam. Black lines are the behavior of σ at small deformations and at the steady state, whose intersection is shown by the circles.

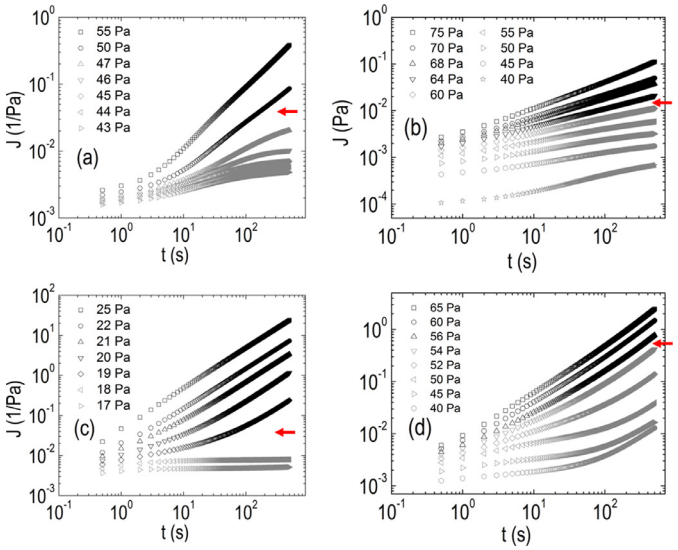

Fig. 6. J vs t obtained from creep measurements for (a) carbopol sample of 0.75 wt%, (b) hair gel, (c) emulsion of 78% vol of oil, and (d) foam. The horizontal arrows indicate the yield stress from the Herschel–Bulkley fit to the steady shear data.

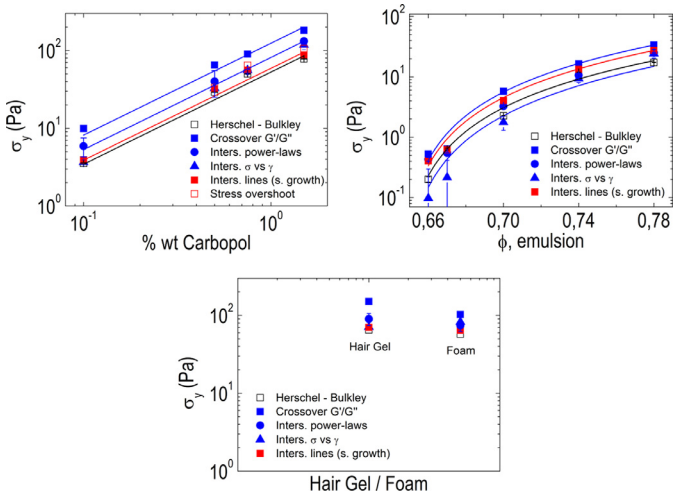

Fig. 7. Yield stress values from different methods for (a) Carbopol, (b) emulsions, and (c) hair gel and foam. Black symbols are the values obtained from steady shear experiments, in which flow curves were fit to the Herschel–Bulkley model. Blue symbols are values obtained from the oscillatory measurements. Red symbols are values obtained from the stress growth experiments. Lines are $\sigma_y \sim (\text{wt\% Carbopol})^{1.18}$ and $\sigma_y \sim (\Delta\phi)^2$, with $\phi_c = 0.645$, for the Carbopol and emulsion, respectively.

to a non-linear elastic response, or it might reflect viscoelasticity; see, for example, [21]. We choose to define the deviation from an elastic response empirically as the intersection between the line with unit slope on logarithmic coordinates that is tangent to the data at low deformations and the horizontal steady-state stress. The former should have a magnitude corresponding to G′, although it is clear from the plots that the line does not pass through the data at the lowest strains.

The use of the maximum in the stress-strain curve to determine both σ_y and γ_y, to the contrary, provides a precise value, but this value is highly dependent on the imposed strain rate and waiting time, as reported by Stokes and Telford [54], Rogers et al. [50], Divoux et al. [22] and Amman et al. [1]. Additionally, a stress overshoot is not always present, as demonstrated by the experiments presented here, where a stress overshoot is only observed for samples with more than 0.5 wt% Carbopol.

Finally, defining σ_y by the steady state gives a precise value of the yield stress, although the value may be dependent on the strain rate, but then the determination of the yield strain is no longer possible.

Creep experiments. Creep data are usually shown as creep compliance $J(t) = \gamma(t)/\sigma$ versus time, where $\gamma(t)$ is the time-dependent shear strain and sigma the constant imposed stress. Creep experiments were carried out within a stress range determined from the results of the previous experiments. In principle, J will go to a constant value at imposed stresses below the yield stress, while it will continue to grow in the liquid state at stresses beyond yielding. Creep compliance data are shown in Fig. 6 for 0.75 wt% Carbopol, the hair gel, 0.78 vol% emulsion, and the foam. The horizontal arrows on the figures indicate the yield stress from the Herschel–Bulkley fit to the steady shear data. The distinction between unyielded and flowing behavior is clear for the Carbopol and the emulsion. It is difficult to identify the location of the change of curvature for the hair gel, although the curvature is clearly different at the lowest and highest stresses. Tabuteau et al. [55] noted in creep measurements on a different Carbopol that there appears to be an intermediate regime in which there is no stable steady flow over the course of the experiment, and it is possible that this behavior is reflected in the hair gel.) The foam data are difficult to interpret because of the upturn at even the small stresses at long times, perhaps because of a change in structure in the unyielded foam; the yield stress is likely given by the apparent loss of an inflection point in the curve.

Overall, conducting creep measurements to find a good estimate of the yield stress appears to be rather inefficient; not only is *a priori* knowledge of the approximate yield stress required, but the method appears to be more sensitive to structural changes during the long time required at a constant stress relative to, for example, a Herschel–Bulkley fit.

3.1.2. Comparison of values obtained from different methods

Yield stress. Fig. 7 shows that different methods do indeed give different yield stress values (error bars correspond to statistical error limits from the fitting parameters). Values obtained from the crossover of G′ and G″ (*characteristic modulus*) are the highest for all cases; this is not surprising, as there is already signif-

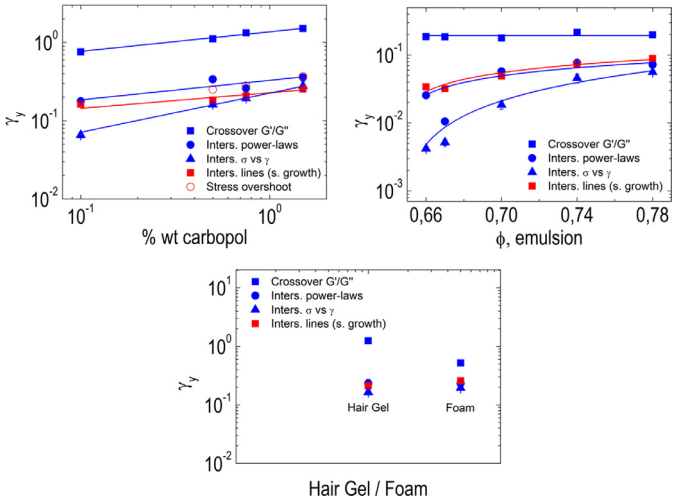

Fig. 8. Yield strain values obtained from different methods for (a) Carbopol, (b) emulsions, and (c) hair gel and foam. Blue symbols are values obtained from the oscillatory measurements. Red symbols are values obtained from the stress growth experiments. Lines represent scaling of γ_y with wt% Carbopol for the Carbopol or $\Delta\phi$ for the emulsions.

icant viscous dissipation by the time that $G' = G''$. Yield stresses obtained from the crossover of G' and G'' are about twice the values obtained from the Herschel–Bulkley model, which are generally the lowest and are close to the transitions seen in the creep experiments for the Carbopol and emulsion. Values obtained from the stress-strain plot derived from the oscillatory data are typically close to the Herschel–Bulkley values, and, as discussed subsequently, these two methods appear to give the most reliable values of the yield stress among those considered here. (This conclusion is consistent with the observation of Christopoulou et al. [18], who identified the intersection of the stress-strain lines as the yield point and the intersection of G' and G'' as the onset of "complete fluidization".) The scaling with concentration is the same for all methods of measurement, however; $\sigma_y \sim (\text{wt\% Carbopol})^{1.18}$ for the Carbopol gels, while, $\sigma_y \sim (\phi - \phi_c)^2$, with $\phi_c = 0.645$, for the emulsion. Previous work Nordstrom et al. [40] has shown similar scaling of σ_y with $\Delta\phi$ for similar systems. The value of $\phi_c = 0.645$ has previously been reported by Paredes et al. [44] for the same system, and is close to the expected value for random close packing, $\phi_{RCP} \approx 0.64$ [10,41,57]; above ϕ_c emulsions jam and a yield stress appears.

Yield strain. Yield strain values obtained with different methods are different, in some cases by an order of magnitude, as shown in Fig. 8 (statistical variations are within the symbols). Yield strains obtained from the characteristic modulus are the highest; as already noted for the yield stress, this is not surprising, as equality of G' and G'' indicates that there has already been a significant amount of dissipation, so the material must have yielded prior to the strain at which $G' = G''$. The values obtained from the stress growth experiments in Fig. 5 are dependent on the particular choice of fitting the low-strain data, and the lines used in all cases have magnitudes equal to only about 80% of G', possibly because of a finite rate effect. Yield strains obtained from the intersection of power-law equations describing the behaviors at low and high γ in oscillatory flow (Fig. 4) are nearly always the lowest; these strains correspond to the yield stresses that are consistent with the fits to the Herschel–Bulkley equation and are probably closest to the true yield strain among the methods studied. Fig. 8 shows that γ_y scales with the amount of polymer for the Carbopol, and with $(\phi - \phi_c) = \Delta\phi$, the distance to jamming, for the emulsion, with $\phi_c = 0.645$, as noted above. These scalings are

Table 1
Scaling of the yield strain with wt% Carbopol for Carbopol samples and ϕ for emulsions.

Rheological measurement	Scaling of γ_y	
	Carbopol	Emulsion
Oscillatory:		
Crossover G' and G'' (Fig. 3)	$\sim (\text{wt\%})^{0.25}$	$\sim \Delta\phi^0$
Intersection power-law equations, G' vs. γ (Fig. 3)	$\sim (\text{wt\%})^{0.25}$	$\sim \Delta\phi^{0.50}$
Intersection power-law equations, σ vs. γ (Fig. 4)	$\sim (\text{wt\%})^{0.50}$	$\sim \Delta\phi^{1.0}$
Stress growth:		
Intersection lines σ vs. γ (Fig. 5)	$\sim (\text{wt\%})^{0.20}$	$\sim \Delta\phi^{0.5}$
Stress overshoot (Fig. 5)	$\sim (\text{wt\%})^{0.37}$	–

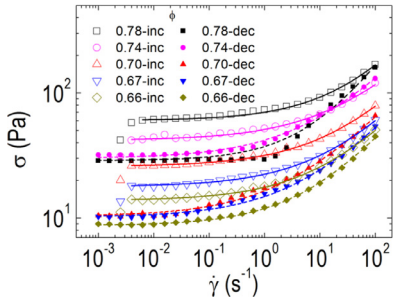

Fig. 9. Increasing and decreasing shear rate sweeps of emulsions with 2 wt% bentonite. Each point was recorded after 10 seconds at the given shear rate. Open symbols are the flow curves going from a low shear rate to a high shear rate, and lines are the fits to the Herschel–Bulkley model. Filled symbols are the flow curves going from a high shear rate to a low shear rate, and dashed lines are the fits to the Herschel–Bulkley model.

shown in Table 1, and it is evident that the scalings are highly dependent on the measuring method; indeed, the results can be different if the same data are analyzed in different ways, as can be seen by comparing the yield strains from oscillatory data obtained by plotting G' vs. γ and σ vs. γ.

3.2. Thixotropic emulsions

The *apparent yield stress* of thixotropic emulsions is determined by applying the same methods used to determine the yield stress of 'simple' yield stress materials. The term *apparent yield stress* is used because, for thixotropic systems, the flow behavior – hence the yield stress – depends on the shear history of the sample, which is why the yield stress is ill-defined for this type of material [25,35]. In particular, all of the methods used here are expected to be sensitive to the rate at which experiments are carried out, as shown, for example, in [23,46].

3.2.1. Rheological measurements

Steady shear measurements. It is evident from the up-and-down flow curves of the loaded emulsions in Fig. 9 that these systems are thixotropic, as hysteresis manifests itself in all of the samples, showing why a single yield stress value cannot be determined. One could indeed define two yield stresses, as done by Mujumdar et al. [36]: a static yield stress, given by fitting the Herschel–Bulkley model to the flow curves going from a low shear rate to a high shear rate, and a dynamic yield stress, given by fitting the same model to the flow curves going from a high to a low shear rate. In all cases, the static yield stress is higher than the dynamic yield stress. Static yield stress measurements to obtain the steady-state flow curve are frequently confounded by viscoelastic effects prior to yielding [23]. As noted in the Introduction, the static yield stress would be the minimum stress needed to start a flow and the dynamic yield stress would be the smallest stress applied before a sample stops flowing.

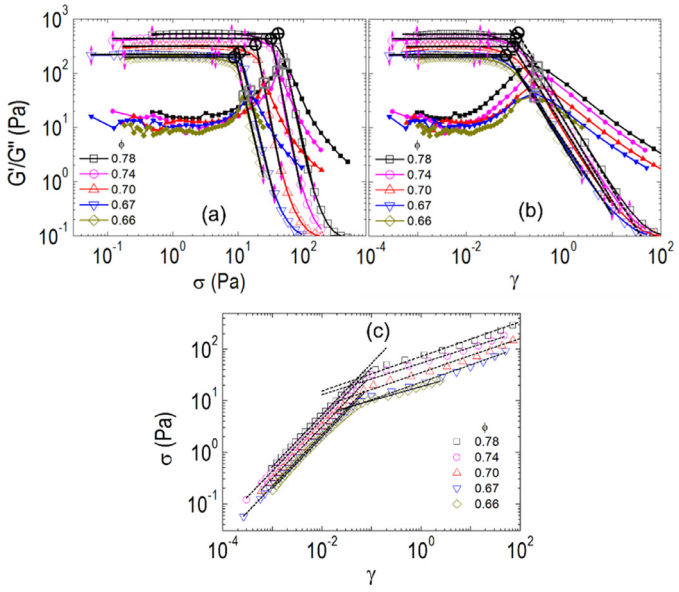

Fig. 10. Oscillatory measurements for emulsions with 2% wt bentonite. (a) G′ and G″ as functions of σ. (b) G′ and G″ as a function of γ. (c) σ as a function of γ. In (a) and (b), open symbols correspond to G′, while filled symbols correspond to G″. (c) is a re-plot of the data shown in (a) and (b). Black lines represent the power-law fits of the behavior of G′ (or σ) well above and well below the yield point. Black circles show σ (or γ) at the intersection of the power-law equations representing the behavior of G′ well above the yield point with the horizontal lines through the linear G′ data. Gray squares show σ (or γ) at the characteristic modulus, where $G' = G''$.

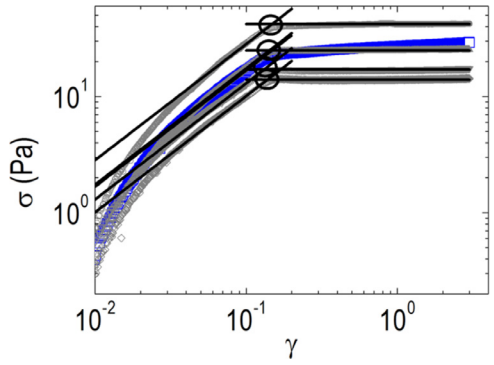

Fig. 11. Shear stress as a function of γ at an imposed $\dot{\gamma} = 1 \times 10^{-2}\ s^{-1}$ for emulsions with 2 wt% bentonite. Blue symbols show the behavior of an emulsion with $\phi = 0.78$. Gray symbols show the behavior of emulsions with $\phi = 0.74$, 0.70, 0.67, and 0.66 (top to bottom). Black lines represent the behavior of σ at small deformations and at the steady state, whose intersection is shown by circles.

Oscillatory measurements. We determined σ_y and γ_y from curves of G′ and G″ vs. σ or γ, shown in Fig. 10(a,b). The same data are re-plotted as σ vs γ, which also allows the determination of σ_y and γ_y (Fig. 10(c)). The crossover of G′ and G″ is a well-defined point, while the behavior of G′ well above the yielding point is poorly described by a power-law equation; hence the intersection of a power-law equation representing the behavior of G′ well above the yield point with the horizontal line through the linear G′ data should not be considered a good method for determining the *apparent yield stress* (or *apparent yield strain*) of the thixotropic samples.

Stress growth experiments. The stress growth experiments are shown in Fig. 11. There is continuous curvature with increasing strain prior to attaining the ultimate steady-state shear stress (save for the emulsion with $\phi = 0.78$, where the stress keeps increasing slightly with the strain even after apparent yielding), so there is no

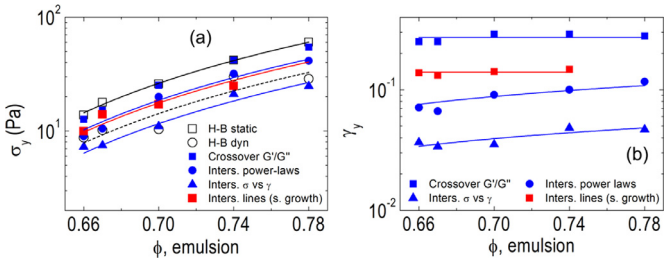

Fig. 12. Behavior of (a) σ_y and (b) γ_y with respect to ϕ for emulsions with 2 wt% bentonite. Black symbols are values obtained from the steady shear experiments, in which flow curves are fit to the Herschel–Bulkley model. Blue symbols are values obtained from the oscillatory measurements. Red symbols are values obtained from the stress growth experiments. Stress growth values of the yield stress and strain are not included for $\phi = 0.78$, since steady state was not reached. All lines correspond to the scalings given in the text.

obvious way to define the yield stress in terms of departure from an elastic response. The yield stress can be determined from the highest stress at which the response is still elastic, the maximum stress, or the steady shear stress. We determine σ_y and γ_y from the intersection of the lines with unit slope on logarithmic coordinates tangent to σ at low deformations and the steady state value of σ (excluding the data at $\phi = 0.78$); the former includes the data in the region just before apparent yielding, with magnitudes equal to about 55% of G′ as measured in the linear viscoelastic oscillatory experiments.

3.2.2. Comparison of values obtained from different methods

Yield stress. Fig. 12(a) shows that different methods give different yield stress values for the thixotropic emulsions, as expected, since the yield stress of these samples is known to be highly dependent on the shear history of the sample. The intersection of the stress-strain curves from the oscillatory measurements and the dynamic yield stress determined from the Herschel–Bulkley fit to the descending shear-rate ramp data are close to each other and give the lowest values. On the other hand, the static yield stress from Herschel–Bulkley fits to the ascending shear-rate ramps and the G′–G″ crossover are close to each another and give the highest values, which are consistent with the value obtained from creep experiments on a sample with slightly different flow curves. The fact that the yield stress obtained from the oscillatory stress-strain curves corresponds to the dynamic yield stress from the flow curves, not the static value, indicates that small-amplitude deformations within the unyielded material have a marked effect on the transition to flow. It is worth noting that all methods for determining an apparent yield stress show the same scaling with concentration, namely $\sigma_y \sim (\phi - \phi_{ct})^2$, with $\phi_{ct} \approx 0.545$; here, ϕ_{ct} denotes a critical volume fraction for the thixotropic system at which the yield stress extrapolates to zero.

Yield strain. Fig. 12(b) shows that yield strain values obtained with different methods are different, but in all cases are relatively insensitive to the volume fraction of clay. Yield strain values obtained from the stress growth experiments and from the characteristic modulus are independent of ϕ, whereas the yield strains obtained from the oscillatory experiments by the intersections of power-law equations above and below yielding, both from G′ and the stress versus strain, roughly follow $\gamma_y \sim (\phi - \phi_{ct})^{0.5}$, with ϕ_{ct} $\phi_{ct} \approx 0.545$. The smallest yield strains are given by the intersection of the high- and low-strain asymptotes for σ v γ obtained from the oscillatory data; the corresponding yield stress is close to that obtained from the Herschel–Bulkley fit to the descending sweep, so this is the yield strain corresponding to the dynamic yield stress. The highest values are given by the intersection of G′ and G″ (the characteristic

Table 2
Overview of rheological measurements and concluding remarks in determining the yield stress.

Rheological measurement	Ambiguity	Remark
Oscillatory:		
Crossover G′ and G″ (Fig. 3)	No	High σ_y, past yielding?
Intersection power-law equations, G′ vs. γ (Fig. 3)	Slope	Definition of crossover point?
Intersection power-law equations, σ vs. γ (Fig. 4)	Slope	Definition of crossover point?
Continuous:		
Intersection lines σ vs. γ (Fig. 5)	Slope	Depends on $\dot{\gamma}$ and waiting time
Stress overshoot (Fig. 5)	Still elastic?	Not always present
Herschel–Bulkley (Fig. 1)	No	Apply low enough $\dot{\gamma}$
Creep (Fig. 6)	No	Inefficient

modulus), for which the corresponding yield stresses correspond to the static yield stresses obtained from the Herschel–Bulkley ascending sweeps.

4. Synthesis and conclusion

The above results clearly show that both the apparent yield strain and the yield stress are dependent on the method and criteria used for determining their values for both normal and thixotropic yield stress materials. In many of the cases studied here the properties determined in different ways exhibit the same scaling with respect to the dispersed phase, albeit with different magnitudes.

For the non-thixotropic yield stress fluids, the value defined by a Herschel–Bulkley fit to a shear-rate sweep consistently gave the lowest yield stress among all methods used. In most cases the intersection between pre-yield and post-yield asymptotes of a stress vs strain curve constructed from oscillatory data gave similar results, and this method consistently gave the lowest value of the yield strain. These values are consistent with each other and, where a valid comparison may be made, with data from the creep experiment. The stress vs strain curve constructed from the oscillatory data generally showed a sharp transition from the linear viscoelastic regime to a power-law response that extended well into the nonlinear regime of substantial dissipation and flow, so it is likely that this transition is close to the point of initiation of flow and provides a good estimate of the yield stress. Hence the Herschel–Bulkley fit and the stress-strain curve from the oscillatory data appear to be the most reliable values among the various methods employed on conventional rheometers, although the former depends on reaching a low enough shear rate and sufficient waiting time to enable reliable extrapolation. The yield stress obtained from stress growth is ambiguous and depends on the time resolution and imposed rate. Generally, determining the yield stress from oscillatory measurements is ambiguous because of the fitting the slopes to find the intersection. The intersection of the G′ and G″ curves as functions of strain (the *characteristic modulus*) is unambiguous but consistently gave the highest values of the yield stress and yield strain; this is to be expected, since the material must have already yielded in order to experience the observed increase in the dissipative modulus G″, and this cannot be considered to be a valid estimate of the yield stress. (In fact, the characteristic modulus was usually close to the maximum of G″ as a function of strain, which is an observation that deserves further exploration.) Table 2 gives an overview of the concluding remarks.

The conclusions for the thixotropic yield stress fluid are similar, except now a static and dynamic yield stress must be considered, as shown in the shear-rate sweeps. The dynamic yield stress determined from the Herschel–Bulkley fit to the descending shear ramp data and the intersection of the stress and strain curves from the oscillatory measurements are close to one another and give the lowest values of the yield stress, and the latter gives the lowest value of the yield strain; the static Herschel–Bulkley fits to the ascending shear-rate ramps and the G′–G″ crossover are close to one another and give the highest values. The finite ramp speed is surely an added factor in the Herschel–Bulkley fits for the thixotropic fluid.

The use of a stress growth curve gives yield stress and yield strain values in most cases that are intermediate, which is undoubtedly a consequence of the ambiguity of the method when there is significant curvature prior to yielding, and this does not appear to be a good method for determining either the static or dynamic yield stress. The same conclusion can be reached for the use of the intersection of high- and low-strain values of G′ in the LAOS experiment.

Supplementary materials

Supplementary material associated with this article can be found, in the online version, at doi:10.1016/j.jnnfm.2016.11.001.

References

[1] C.P. Amman, M. Siebenburger, M. Kruger, F. Weysser, M. Ballauff, M. Fuchs, Overshoots in stress-strain curves: colloid experiments and mode coupling theory, J. Rheol. 57 (2013) 149–175.
[2] M.J. Armstrong, A.N. Beris, S.A. Rogers, N.J. Wagner, Dynamic shear rheology of a thixotropic suspension: comparison of an improved structure-based model with large amplitude oscillatory shear experiments, J. Rheol. 60 (2016) 433–450.
[3] N.J. Balmforth, I.A. Frigaard, G. Ovarlez, Yielding to stress: recent developments in viscoplastic fluid mechanics, Annu. Rev. Fluid Mech. 46 (2014) 121–146.
[4] H.A. Barnes, Thixotropy - a review, J. Non-Newton. Fluid Mech. 70 (1997) 1–33.
[5] H.A. Barnes, The yield stress – a review or '$\pi\alpha\nu\tau\alpha\ \rho\epsilon\iota$' – everything flows? J. Non-Newton. Fluid Mech. 81 (1999) 133–178.
[6] H.A. Barnes, J.F. Hutton, K. Walters, An Introduction to Rheology, Elsevier Science Publishers B. V., 1989.
[7] H.A. Barnes, Q.D. Nguyen, Rotating vane rheometry—a review, J. Non-Newton. Fluid Mech. 98 (2001) 1–14.
[8] H.A. Barnes, K. Walters, The yield stress myth? Rheol. Acta 24 (1985) 323–326.
[9] B.C. Blackwell, R.H. Ewoldt, A simple thixotropic-viscoelastic constitutive model produces unique signatures in large-amplitude oscillatory shear (LAOS), JNNFM 208 (2014) 27–41.
[10] J.D. Bernal, J. Mason, Packing of spheres: co-ordination of randomly packed spheres, Nature 188 (1960) 910–911.
[11] V. Bertola, F. Bertrand, H. Tabuteau, D. Bonn, P. Coussot, Wall slip and yielding in pasty materials, J. Rheol. 47 (2003) 1211–1226.
[12] E.C. Bingham, Fluidity and Plasticity, McGraw-Hill, New York, 1922.
[13] R.B. Bird, D. Gance, B.J. Jarusso, The rheology and flow of viscoplastic materials, Rev. Chem. Eng. 1 (1983) 1–70.
[14] D. Bonn, M.M. Denn, Yield stress fluids slowly yield to analysis, Science 324 (2009) 1401–1402.
[15] S. Clayton, T.G. Grice, D.V. Boger, Analysis of the slump test for on-site yield stress measurement of mineral suspensions, Int. J. Miner. Process. 70 (2003) 3–21.
[16] P. Coussot, Yield stress fluid flows: a review of experimental data, J. Non-Newton. Fluid Mech 211 (2014) 31–49.
[17] P. Coussot, Q.D. Nguyen, H.T. Huynh, D. Bonn, Viscosity bifurcation in thixotropic, yielding fluids, J. Rheol. 46 (2002) 573–589.
[18] C. Christopoulou, G. Petekides, B. Erwin, M. Cloitre, D. Vlassopoulos, Ageing and yield behavior in model soft colloidal glasses, Phil. Trans. Roy. Soc. A 367 (2009) 5051–5071.
[19] F. Cyriac, P.M. Lugt, R. Bosman, On a new method to determine the yield stress in lubricating grease, Tribol. Lubricat. Technol. 72 (2016) 60–72.
[20] V. De Graef, F. Depypere, M. Minnaert, K. Dewettinck, Chocolate yield stress as measured by oscillatory rheology, Food Res. Int. 44 (2011) 2660–2665.

[21] M.M. Denn, D. Bonn, Issues in the flow of yield-stress liquids, Rheol. Acta 50 (2011) 307–315.
[22] T. Divoux, C. Barentin, S. Manneville, Stress overshoot in a simple yield stress fluid: an extensive study combining rheology and velocimetry, Soft Matter 7 (2011) 9335–9349.
[23] T. Divoux, V. Grenard, S. Manneville, Rheological hysteresis in soft glassy materials, Phys. Rev. Lett. 110 (2013) 018304.
[24] R.H. Ewoldt, A.E. Hosoi, G.H. McKinley, New measure for characterizing nonlinear viscoelasticity in large amplitude oscillatory shear, J. Rheol. 52 (2008) 1427–1458.
[25] A. Fall, J. Paredes, D. Bonn, Yielding and shear banding in soft glassy materials, Phys. Rev. Lett. 105 (2010) 225502.
[26] W. Herschel, R. Bulkley, Measurement of consistency as applied to rubber-benzene solutions, Proc. Am. Assoc. Test Mater. 26 (1926) 621–633.
[27] K. Hyun, M. Wilhelm, C. Klein, K. Cho, J. Nam, K. Ahn, S. Lee, R. Ewoldt, G. McKinley, A review of nonlinear oscillatory shear tests: analysis and application of large amplitude oscillatory shear (laos), Progress Polymer Sci. 36 (2011) 1697–1753.
[28] A.E. James, D.J.A. Williams, P.R. Wiliams, Direct measurement of static yield properties of cohesive suspensions, Rheol. Acta 26 (1987) 437–446.
[29] C. Kugge, N. Vanderhoek, D.W. Bousfield, Oscillatory shear response of moisture barrier coatings containing clay of different shape factor, J. Colloid Interface Sci. 358 (2011) 25–31.
[30] R.G. Larson, The Structure and Rheology of Complex Fluids, Oxford University Press, Inc., 1999.
[31] T.G. Mason, J. Bibette, D.A. Weitz, Yielding and flow of monodisperse emulsions, J. Colloid Interface Sci. 179 (1996) 439–448.
[32] J. Mewis, A.J.B. Spaull, Rheology of concentrated dispersions, Adv. Colloid Interface Sci. 6 (1976) 173–200.
[33] P.C.F. Møller, A. Fall, D. Bonn, Origin of apparent viscosity in yield stress fluids below yielding, Europhys. Lett. 87 (2009) 38004.
[34] P.C.F. Møller, J. Mewis, D. Bonn, Yield stress and thixotropy: on the difficulty of measuring yield stresses in practice, Soft Matter 2 (2006) 274–283.
[35] P. Møller, A. Fall, V. Chikkadi, D. Derks, D. Bonn, An attempt to categorize yield stress fluid behavior, Phil. Trans. Roy. Soc. A 367 (2009) 5139–5155.
[36] A. Mujumdar, A.N. Beris, A.B. Metzner, Transient phenomena in thixotropic systems, J. Non-Newton. Fluid Mech. 102 (2002) 157–178.
[37] Q.D. Nguyen, T. Akroyd, D.C.D. Kee, L. Zhu, Yield stress measurements in suspensions: an inter-laboratory study, Korea-Aust. Rheol. J. 18 (2006) 15–24.
[38] Q.D. Nguyen, D.V. Boger, Yield stress measurements for concentrated suspensions, J. Rheol. 27 (1983) 321–349.
[39] Q.D. Nguyen, D.V. Boger, Measuring the flow properties of yield stress fluids, Annu. Rev. Fluid Mech. 24 (1992) 47–88.
[40] K.N. Nordstrom, E. Verneuil, P.E. Arratia, A. Basu, Z. Zhang, A.G. Yodh, J.P. Gollub, D.J. Durian, Microfluidic rheology of soft colloids above and below jamming, *Phys. Rev. Lett*. 105 (2010) 175701.
[41] E.R. Nowak, J.B. Knight, E. Ben-Naim, H.M. Jaeger, S.R. Nagel, Density fluctuations in vibrated granular materials, Phys. Rev. E 57 (1998) 1972–1982.
[42] G. Ovarlez, S. Cohen-Addad, K. Krishnan, J. Goyon, P. Coussot, On the existence of a simple yield stress behavior, J. Non-Newton. Fluid Mech. 193 (2013) 68–79.
[43] G. Ovarlez, L. Tocquer, F. Bertrand, P. Coussot, Rheopexy and tunable yield stress of carbon black suspensions, Soft Matter 9 (2013) 5540–5549.
[44] J. Paredes, M.A.J. Michels, D. Bonn, Rheology across the zero-temperature jamming transition, Phys. Rev. Lett. 111 (2013) 015701.
[45] J. Paredes, N. Shahidzadeh-Bonn, D. Bonn, Shear banding in thixotropic and normal emulsions, J. Phys. Condens Mat. 23 (2011) 284116.
[46] C. Perge, N. Taberlet, T. Gibaud, S. Manneville, Time dependence in large amplitude oscillatory shear: a rheoultrasonic study of fatigue dynamics in a colloidal gel, J. Rheol. 58 (2014) 1331–1357.
[47] J.M. Piau, Carbopol gels: elastoviscoplastic and slippery glasses made of individual swollen sponges. Meso- and macroscopic properties, constitutive equations and scaling laws, J. Non-Newton. Fluid Mech 144 (2007) 1–29.
[48] A. Ragouilliaux, G. Ovarlez, N. Shahidzadeh-Bonn, B. Herzhaft, T. Palermo, P. Coussot, Transition from a simple yield-stress fluid to a thixotropic material, Phys. Rev. E 76 (2007) 051408.
[49] F. Renou, J Stellbrink, G Peterkidis, Yielding processes in a colloidal glass of soft star-like micelles under large amplitude oscillatory shear (LAOS), J. Rheol. 54 (2010) 1219–1242.
[50] S.A. Rogers, P.T. Callaghan, G. Petekidis, D.V. Vlassopoulos, Time-dependent rheology of colloidal star glasses, J. Rheol. 54 (2010) 133–158.
[51] S.A. Rogers, B.M. Erwin, D. Vlassopoulos, M. Cloitre, A sequence of physical processes determined and quantified in laos: application to a yield stress fluid, J. Rheol. 55 (2011) 435–458.
[52] F. Rouyer, S. Cohen-Addad, R. Höhler, Is the yield stress of aqueous foam a well-defined quantity? Colloid Surface. A 263 (2005) 111–116.
[53] A. Saint-Jalmes, D.J. Durian, Vanishing elasticity for wet foams: equivalence with emulsions and role of polydispersity, J. Rheol. 43 (1999) 1411–1422.
[54] J. Stokes, J. Telford, Measuring the yield behaviour of structured fluids, J. Non-Newton. Fluid Mech. 124 (2004) 137–146.
[55] H. Tabuteau, P. Coussot, J.R. de Bruyn, Drag force on a sphere in steady motion through a yield-stress fluid, *J. Rheol*. 51 (2007) 125–137.
[56] M.U. Vera, A. Saint-Jalmes, D.J. Durian, Scattering optics of foam, Appl. Optics 40 (2001) 4210–4214.
[57] D.A. Weitz, Packing in the spheres, Science 303 (2004) 968–969.
[58] A. Yoshimura, R.K. Prud'homme, Wall slip corrections for couette and parallel disk viscometers, J. Rheol 32 (1988) 53–67.
[59] L. Zhu, N. Sun, K. Papadopoulos, D. De Kee, A slotted plate device for measuring static yield stress, J. Rheol. 45 (2001) 1105.